Friction and wear performance of electrospark deposited Ni/C-MoS_2 self-lubricating coating

F. L. Kong[a,b], L. Zhang[c], W. J. Zhao[d], D. S. Zheng[b], T. J. Sui[b], G. L. Zhu[a], C. A. Guo[a,*]

[a]*School of Equipment Engineering, Shenyang Ligong University, Shenyang 110159, China*

[b]*Norinco Group Air Ammunition Research Institute Co.,Ltd., Haerbin 15001, China*

[c]*North Huaan Industry Group Co. Ltd, Qiqihaer 161046, China*

[d]*Liaoshen lndusteries Croup Co. Ltd, Shenyang 110045, China*

A Ni/C-MoS_2 coating was electrospark deposited by using an electrode made of sinered Ni-C-MoS_2 composite on a CrNi3MoVA steel substrate, and its nano-mechanical properties and tribological properties were obtained by utilizing nano-indenter and friction-abrasion testing machine. The results showed that the phase constitution of the as-deposited Ni/C-MoS_2 coating mainly includes graphite, MoS_2, γ-Ni, MoO_2, Ni_xS and MoC. Compared with the CrNi3MoVA steel and Ni/MoS_2 coating, the Ni/C-MoS_2 coating exhibits better tribological properties due to the matrix strengthened by MoO_2 and MoC, and the synergistic lubrication effect of graphite and MoS_2 in the Ni/C-MoS_2 coating.

(Received June 3, 2024; August 28, 2024)

Keywords: Self-lubricating coating, Electrospark deposition, Graphite, MoS_2, Friction and wear

1. Introduction

Surface wear will lead to premature failure of the components, and then lead to abnormal working of the whole equipment. According to incomplete statistics, 1/3~1/2 of the energy was consumed duo to wear. Wear is the main form of failure, and about 80% of the failure of the mechanical components is caused by wear [1]. Therefore, it is especially important to enhance the tribological properties of the pivotal parts of equipment. Solid lubricants can remain anti-friction under dry serve condition and be applied in environments where liquid lubricants cannot be used, such as hot or cryogenic environment, vacuum, radiation and high pressure. At present, most single lubricants have good lubrication effect under specific conditions, but materials with good lubrication capability in all kinds of environments are rare.

MoS_2 is one of the most used solid lubricants in the world for it possesses good lubrication performance in low-speed and dry condition. However, most of MoS_2 is transformed into MoO_3 after it is in wet air for a long time, and then the lubrication layer will be damaged, resulting in a sharp decline in lubrication performance [2]. Yang J et al. [3] prepared Ni/MoS_2 coating with high bonding strength and good surface morphology by electrospark deposition (ESD) technology, showing that the Ni/MoS_2 coating possesses outstanding tribological performance in atmospheric environment for the coefficient of friction (COF) and wear rate reduced 75% and 46% respectively comparison to the uncoated steel substrate. When studying the lubrication and wear performance of solid lubrication coating system, it is found that the synergistic effect of a variety of solid lubricants can offset the defects of the coating caused by using a single solid lubricant. Some scholars [4-7] have found that MoS_2 has a good synergistic effect with graphite. When MoS_2 and graphite are used at the same time, the friction and wear properties are significantly improved compared with MoS_2 or graphite alone. In this work, a Ni/C-MoS_2 coating is fabricated by ESD technology and its friction and wear properties will be studied.

* Corresponding author: bigocean1979@aliyun.com

https://doi.org/10.15251/CL.2024.218.665

2. Materials and methods

The Ni-C-MoS_2 composite was fabricated by spark plasma sintering technique. The 50 Wt.% Nickel powder, 10 Wt.% graphite powder and 40 Wt.% MoS_2 powder were mixed, and then they were loaded into graphite mold and sintered in vacuum in the furnace. The powder mixture was heated from room temperature to 1100 ℃ at a speed of 50 ℃/min, and then sintered at a constant temperature of 1050 ℃ under a pressure of 40 MPa for 20 min, and after that cooled in the furnace.

The CrNi3MoVA steel (chemical composition: 0.40 Wt.% C, 0.41 Wt.% Mn, 0.25 Wt.% Si, 1.28 Wt.% Cr, 3.14 Wt.% Ni, 0.37 Wt.% Mo, 0.20 Wt.% V, 0.001 Wt.% S, 0.012 Wt.% P balanced Fe) [8] was used as the substrate. The substrate material with a dimension of 30 mm×20 mm×5 mm and the Ni/C-MoS_2 composite electrode with a diameter of 5 mm and a length of 50 mm were ground with SiC sandpapers step by step to 1500 particle, and then they were put into the mixture of ethanol and acetone for ultrasonic cleaning for 30 min. Finally, they were taken out with tweezers and immediately dried with a hair dryer.

The Ni/C-MoS_2 coatings were fabricated on the CrNi3MoVA steel samples by a DJ-2000 ESD machine. Argon was used for protection during ESD process, and the optimum process parameters of ESD were as follows: the power was 1200 W, the Ar gas flow speed 15 $L \cdot min^{-1}$, the electrode rotating speed 3500 $r \cdot min^{-1}$, the deposition time per area 2 $min \cdot cm^{-1}$, and the voltage 80 V. For comparison, the Ni/MoS_2 coating was also prepared in reference [3].

The hardness and elastic modulus were tested by employing a Berkovich nano-indenter G200, and those of Oliver Farr model were calculated through the loading curves. The values of the hardness and elastic modulus of the samples were the average values of eight points parallel to the surface of the coating on the cross section. The tribological properties were obtained by using an MFT-5000 friction and wear tester. The schematic of the friction and wear experiment of the coatings displays in Figure 1, and the conditions were as follows: the grinding head was an Al_2O_3 ball, its diameter 8 mm, the distance 6 mm, the speed 50 mm/s, the load 10 N, and the total rubbing time 10 min.

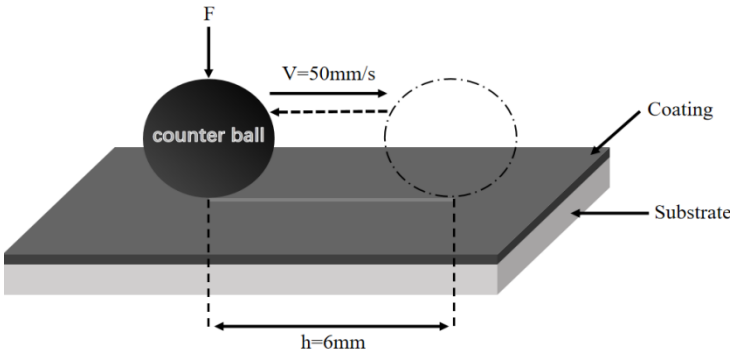

Fig. 1. Schematic of friction and wear experiment of the coating.

The original and worn morphologies of the samples were characterized by scanning electron microscopy, and the chemical composition of the selected areas of the Ni/C-MoS_2 coating was obtained by energy-dispersive spectrometer. The phase structure of the Ni/C-MoS_2 coating was analyzed by X-ray diffraction.

3. Results and discussion

3.1. Microstructure of Ni/C-MoS_2 coating

Figure 2 displays the surface morphology of the ESD Ni/C-MoS_2 coating. As shown in Figure 2, one zone of the Ni/C-MoS_2 coating surface presents a smooth liquid flow feature, which is due to the melting of the electrode at an instantaneous high temperature of electrospark discharge, and then the micro-molten material solidifies at a very high cooling speed. The other zone of the surface is formed by agglomeration and accumulation of granular materials showing rough cauliflower shape. Overall, the coating surface is dense without obvious cracks.

Figure 3 displays the EDS results of area A and B in Figure 2 respectively. The EDS results in area A (Figure 3(a)) on the Ni/C-MoS_2 coating show that although the ESD process was protected by argon flow, the coating was still oxidized. The ratio of S to Mo is less than 2:1, indicating that the loss of S takes place in the ESD process. Figure 3(b) shows the EDS results in area B on the Ni/C-MoS_2 coating. Different from area A, a large amount of C is detected in area B, indicating that the agglomerated surface particles may be graphite. The content of other metal elements, such as Ni and Mo, is a small quantity in zone B, and O is also detected on the surface of area B. In addition, a small amount of Fe is also detected in area A and area B, indicating that the substrate elements diffuse into the coating, and the bonding between the coating and the substrate is good.

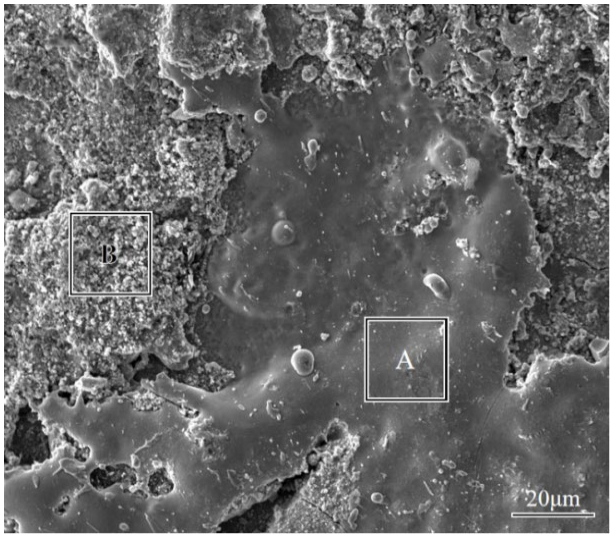

Fig. 2. Surface morphology of the ESD Ni/C-MoS_2 coating.

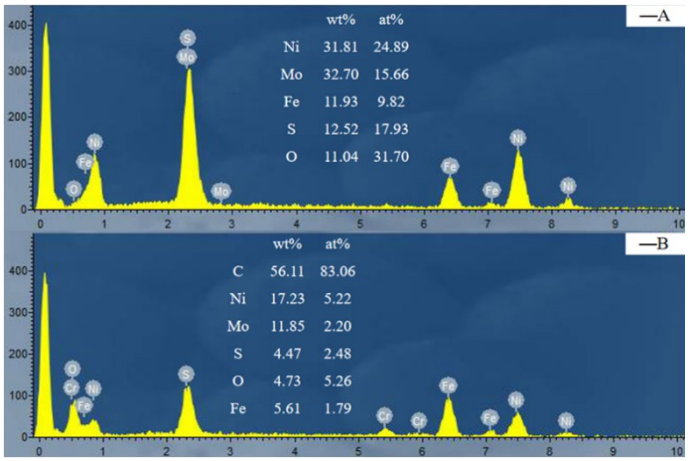

Fig. 3. EDS results of area A and B of the ESD Ni/C-MoS_2 coating.

Figure 4 displays the cross-sectional morphology (a) and EDS line scanning results (b) of the ESD Ni/C-MoS_2 coating. The interface between the coating and the substrate can be clearly distinguished as shown in Figure 4 (a). The inside microstructure of the coating without cracks is dense, and the thickness of the coating is about 70 μm. The top layer of the coating cross-section shows a darker color, which may be due to the high content of the graphite on the surface of the coating for it has a low density. The EDS line scanning results from the top of the Ni/C-MoS_2 coating to the substrate in Figure 4 (b) show that the content of C element is the highest on the coating surface, and it is evenly distributed in the depths of the coating, which is also consistent with the dark area on the top layer of the coating. In addition, the content gradient of Fe about 10 μm indicates that it diffuses from the substrate into the coating, resulting in an excellent metallurgical bond between the coating and the substrate.

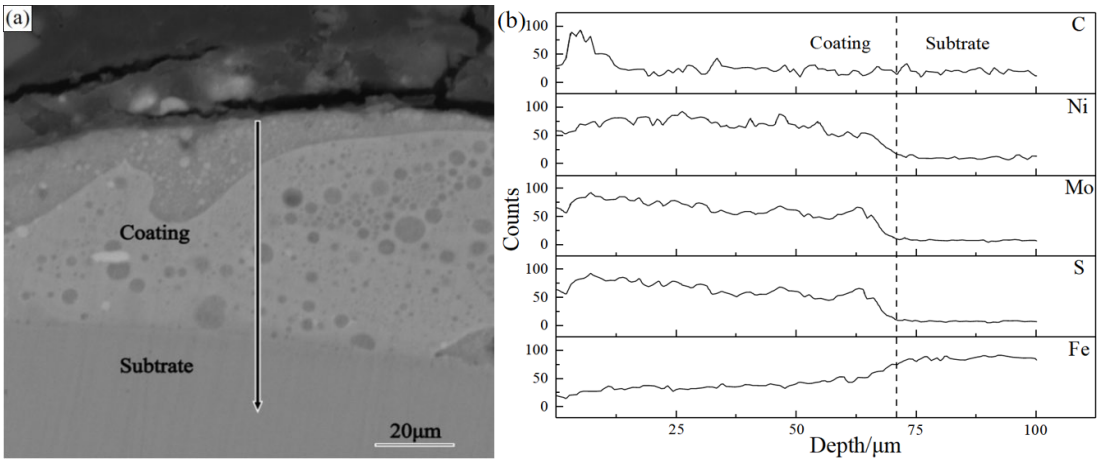

Fig. 4. Cross sectional morphology (a) and EDS line scanning (b) of the ESD Ni/C-MoS_2 coating.

Figure 5 displays the XRD pattern of the ESD Ni/C-MoS_2 coating. As displayed in Figure 5, the phase structure of the Ni/C-MoS_2 coating mainly consists of graphite, MoS_2, γ-Ni, MoO_2, Ni_xS and MoC. Ni_xS is used here for the peaks of NiS and Ni_3S_2 are both detected. In the range of partial diffraction angles, the typical amorphous peaks and wide peaks appear in the spectrum, which indicates that the grains of the coating are refined and some amorphous structures are formed in the ESD process.

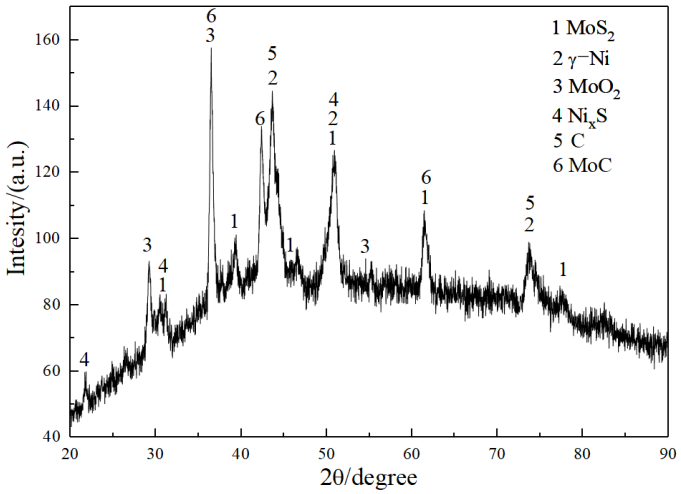

Fig. 5. XRD pattern of the ESD Ni/C-MoS_2 coating

According to the EDS and XRD results of the Ni/C-MoS_2 coating, mixing O_2 in the ESD process may lead to three reactions:

$$MoS_2+2Ni+O_2=MoO_2+2NiS$$
$$MoS_2+3Ni+O_2=MoO_2+Ni_3S_2$$
$$Mo+C=MoC \quad (1)$$

where Mo in the reaction comes from the decomposition of MoS_2 at high temperature. Thermodynamic calculation can be used to judge whether the three reactions can be carried out spontaneously, so as to verify the correctness of the XRD analysis.

According to the Gibbs free energy (G) of each substance, the G at the corresponding temperature (T) of the three groups of reaction equation is calculated, as shown in Table 1.

Table 1. Gibbs free energy of reactions at some temperatures.

Temperature T/(K)	298	400	600	800	1000
ΔG_1/(kJ/mol)	-466.6	-448.76	-413.48	-378.64	-334.48
ΔG_2/(kJ/mol)	-440.94	-422.86	-386.9	-350.06	-312.74
ΔG_3/(kJ/mol)	-10.03	-10.12	-10.72	-11.94	-13.41

Fitted by linear regression method, the relationship between G and T is as follows:

$$\Delta G_1 = -523.49+0.1858T \text{ kJ/mol}$$
$$\Delta G_2 = -495.85+0.1826T \text{ kJ/mol}$$
$$\Delta G_3 = -8.67-0.858T \text{ kJ/mol} \quad (2)$$

It can be concluded from the functional relationship that the reaction in the ESD process is negative below 2700 K, and MoO_2, MoC and Ni_xS may be formed. At high temperature, Mo from MoS_2 reacts with C and O_2 respectively to form a certain amount of MoC and MoO_2 in the coating. MoC has a high fusion point (2615 ℃) and a high hardness (1400 HV) comparison to general metal carbides. Furthermore, it has good thermal stability, mechanical stability and corrosion resistance. MoO_2 also has a high fusion point (2600 ℃) and a high hardness (1100 HV). Both MoC and MoO_2 together act as dispersion strengthening (DS) phases to increase the hardness of the coating.

3.2. Nano-mechanical properties of Ni/C-MoS_2 coating

Table 2 displays the nano-mechanical properties of the CrNi3MoVA steel, ESD Ni/MoS_2 coating and Ni/C-MoS_2 coating. As displayed in Table 2, the hardness of the Ni/C-MoS_2 coating is 6.23 GPa and its elastic modulus is 139.7 GPa. Compared with the CrNi3MoVA steel and Ni/MoS_2 coating, the hardness of the Ni/C-MoS_2 coating increases about 37% and 24% respectively. This is mainly due to the following reasons: firstly, the grains of the coating are refined, and the fine grains and amorphous structure have higher hardness due to ultra-high cooling speed during the ESD process [9-10]; secondly, compared with Ni/MoS_2 coating, although the addition of the soft graphite phase in the Ni/C-MoS_2 coating will reduce the hardness of the coating, graphite reacts with Mo to form ceramic phase MoC, which makes the Ni/C-MoS_2 coating have higher hardness comparison to the Ni/MoS_2 coating.

Table 2. Nano-mechanical properties of CrNi3MoVA steel, ESD Ni/C-MoS_2 coating and Ni/MoS_2 coating.

Sample	Hardness H(GPa)	Elastic modulus E(GPa)	H/E	H^3/E^2
CrNi3MoVA steel	4.54	264.5	0.017	0.0013
Ni/MoS_2 coating	5.03	144.7	0.035	0.0061
Ni/C-MoS_2 coating	6.23	139.7	0.045	0.0124

Other important parameters for predicting the service life of samples can also be obtained from nano-indentation results. Hardness is not necessarily the most important factor affecting coating wear resistance, and elasticity and toughness are also important factors, especially in wear. The coating tribological performance cannot be described only by hardness, but by the ratio of hardness to elastic modulus, namely H/E value [11]. The H/E value decides the elastic behavior limit of the friction contact surface. The number of convex or concave body, whose stress exceeds its elastic limit on the worn surface, decreases with the increase of H/E value, and the material with high H/E value can elastically recover the deformation caused by external load, so as to reduce the friction of sliding contact and improve the wear resistance. In this work, the H/E value of the Ni/C-MoS_2 coating is about 264% and 29% higher comparison to the CrNi3MoVA steel and Ni/MoS_2 coating respectively, indicating that the Ni/C-MoS_2 coating exhibits the best wear resistance.

Research shows that another important material characteristic, contact yield pressure, can also be described by measuring hardness and elastic modulus when the geometry of the contact object is known [12]. For example, the formula for the yield pressure of an elastic-plastic plate in contact with a rigid ball is:

$$P_y = 0.78r^2\left(\frac{H^3}{E^2}\right) \tag{3}$$

where r is the radius of the contact ball. Therefore, H^3/E^2 value is another parameter relating to wear characteristics [13], and it represents the ability of the material to resist plastic deformation against contact load, namely yield pressure. The H^3/E^2 value of the Ni/C-MoS_2 coating is about 954% and 203% higher comparison to the CrNi3MoVA steel and Ni/C-MoS_2 coating respectively, which suggests that the Ni/C-MoS_2 coating has the best tribological property.

3.3. Friction and wear behavior of Ni/C-MoS_2 coating

Figure 6 displays the worn morphology of the ESD Ni/C-MoS_2 coating. As shown in Figure 6, the worn morphology is similar as the original morphology of the Ni/C-MoS_2 coating, which is also divided into the dark smooth zones and the light particle agglomeration zones. The content of metal elements with smooth morphology is high, which is the metal matrix of the coating, providing wear resistance for the coating during rubbing. The MoO_2, MoC dispersion strengthened phases generated in the ESD process make the smooth zone have very high hardness. After rubbing, except that there are only slight scratches, the original smooth surface of the coating is relatively flat without cracks and spalling. Therefore, the wear mechanism of the Ni/C-MoS_2 coating mainly belongs to slight abrasive wear. However, it can be observed that the original convex position was ground flat. Combined with the EDS results, it can be seen that the cauliflower-like area contains a large amount of solid lubricating composition. When the rubbing starts, the smooth area with high hardness provides support for the whole coating. The granular lubricant is squeezed into the concaves under pressure, and then gradually forms a smooth and continuous lubricating film under the reciprocating motion between friction pair. Besides small friction contact area can effectively reduce the COF and improve the wear resistance of the coating. The matrix structure with high hardness makes the lubricating film not produce fatigue failure prematurely under load, prolonging the fatigue life of the lubricating interface and reducing the COF.

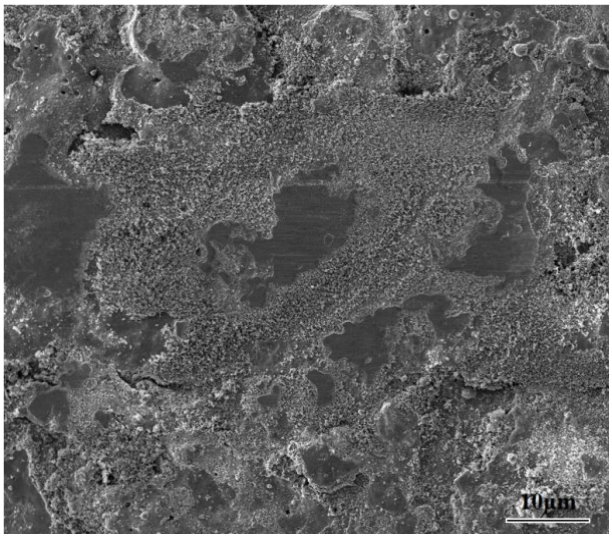

Fig. 6. Worn morphology of the ESD Ni/C-MoS_2 coating.

Figure 7 displays the COFs of the CrNi3MoVA steel, ESD Ni/C-MoS_2 coating and Ni/MoS_2 coating. In the initial rubbing stage, due to the uneven surface morphology and lubricating materials distributed on the coating, the COF of the Ni/C-MoS_2 coating is not stable, showing a running period; then with the support of the hard matrix structure in the coating and the formation of the lubricating film, the Ni/C-MoS_2 coating shows a low and stable COF. The COF of the Ni/C-MoS_2 coating is about 0.17, which is about 77% and 45% lower comparison to the CrNi3MoVA steel and Ni/MoS_2 coating respectively. During the rubbing process, the accumulated rubbing heat tends to lead to the volatilization and oxidation of some MoS_2, resulting in lubrication performance reduction of the Ni/MoS_2 coating. During the rubbing process of the Ni/C-MoS_2 coating, the high temperature resistance of graphite ensures that it can still provide good lubrication effect for the coating even after the MoS_2 content is reduced. The metal matrix with high hardness guarantees that the Ni/C-MoS_2 coating can still form a continuous and complete lubrication film against the Al_2O_3 ball with high hardness.

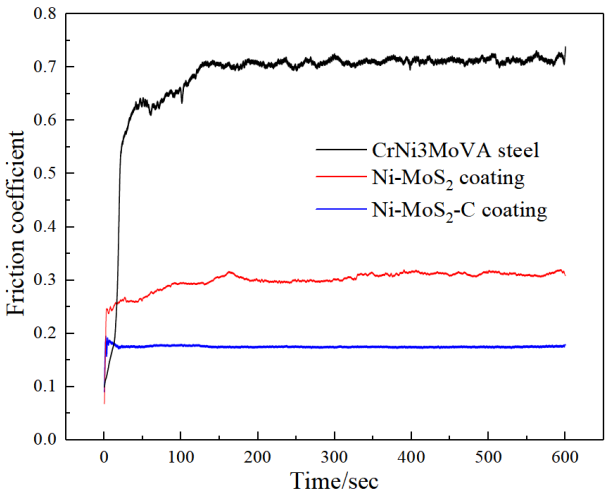

Fig. 7. COFs of CrNi3MoVA steel, ESD Ni/C-MoS_2 coating and Ni/MoS_2 coating.

The worn volume can be accurately calculated through the worn trace width L and the diameter d of Al_2O_3 ball in Figure 8, and the volume wear rate can be further obtained [14]. The calculation formula of the volume wear rate is:

$$W = \frac{\arcsin(\frac{L}{d}) \times \pi d^2 - 180 \times L \times \sqrt{d^2 - L^2}}{720 \times F \times v \times t} \times h \tag{4}$$

where W is the volume wear rate, d the diameter of Al_2O_3 ball (8 mm), h the wear trace length (6 mm), L the worn trace width (mm), F the load (10 N), v the rubbing speed (5×10^{-2} m/s), and t the rubbing time (600 s). The worn trace width of the CrNi3MoVA steel and the coating can be clearly observed through the SEM images (Figure 9), and the volume wear rate is calculated as shown in Figure 10.

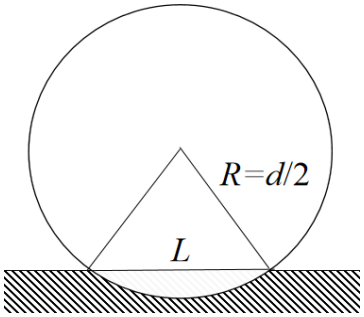

Fig. 8. Wear volume diagram.

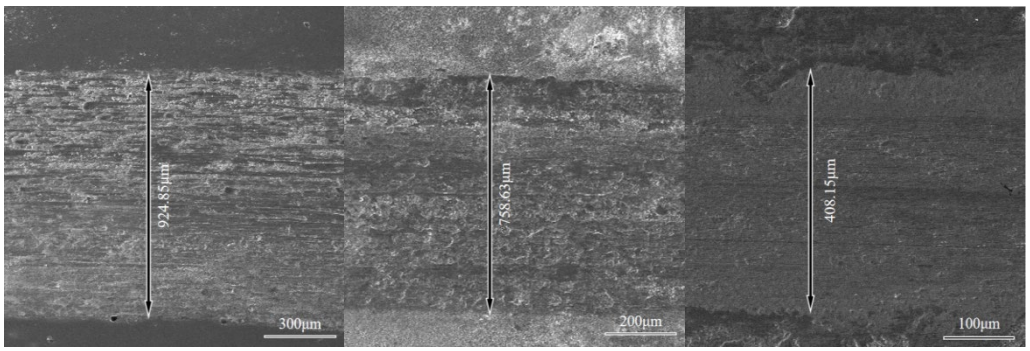

Fig. 9. Worn trace of CrNi3MoVA steel, Ni/MoS_2 coating and Ni/C-MoS_2 coating.

As shown in Figure 10, the wear rate of the Ni/C-MoS_2 coating is 2.89×10^{-5} $mm^3 \cdot N^{-1} \cdot m^{-1}$, about 91% and 84% lower comparison to the CrNi3MoVA steel and Ni/MoS_2 coating respectively. In this work, the Al_2O_3 ball has higher hardness and lower metallurgical compatibility to the coating comparison to the GCr15 steel, so it tends to produce abrasive wear instead of adhesive wear. The MoO_2, MoC dispersion strengthened phases generated in the ESD process significantly improve the mechanical properties of the matrix in the coating. Moreover, the synergistic effect of graphite and MoS_2 in the concave zones of the coating notably reduce the COF of the coating and further enhance the wear resistance.

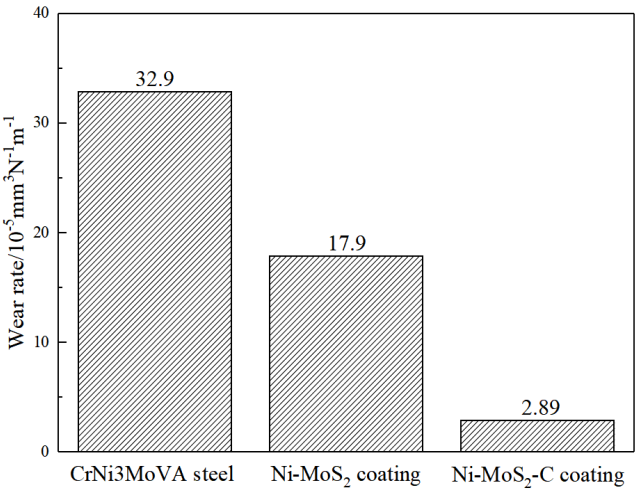

Fig. 10. Wear rate of CrNi3MoVA steel, Ni/MoS_2 coating and Ni/C-MoS_2 coating.

4. Conclusions

The phase structure of the ESD Ni/C-MoS_2 coating is composed of graphite, MoS_2, γ-Ni, MoO_2, Ni_xS, and MoC, and the coating consists of the matrix zones strengthened by MoO_2, MoC dispersion phases and agglomeration and accumulation of granular zones as lubrication materials. The hardness of the Ni/C-MoS_2 coating is about 37% and 24% higher, and its elastic modulus is about 47% and 3% lower comparison to the CrNi3MoVA steel and Ni/MoS_2 coating respectively. The COF of the Ni/C-MoS_2 coating is about 0.17, which is about 77% and 45% lower comparison to the CrNi3MoVA steel and Ni/MoS_2 coating, and the wear rate is 2.89×10^{-5} $mm^3 \cdot N^{-1} \cdot m^{-1}$, which is about 91% and 84% lower comparison to the CrNi3MoVA steel and Ni/MoS_2 coating respectively.

Acknowledgments

The authors are grateful for the financial support of the Research Project of Application Foundation of Liaoning Province of China (No.2022JH2/101300006), the Special Fund of Basic Scientific Research Operating Expense of Undergraduate Universities in Liaoning Province, the Guangxuan Team Plan of SYLU, and the Foundation of National Key Laboratory for Remanufacturing.

References

[1] P. J. Blau, Friction science and technology: from concepts to applications, CRC press, (2008); https://doi.org/10.1201/9781420054101

[2] S. Zhang, G. L. Li, H. D. Wang, B. S. Xu, G. Z. Ma, Physics Procedia 50, 199 (2013); https://doi.org/10.1016/j.phpro.2013.11.032

[3] C. Guo, F. Kong, S. Zhao, X. Yan, J. Yang, J. Zhang, Chalcogenide Letters 16(7), 309 (2019).

[4] J. L. Li, D. S. Xiong, Wear 265, 533 (2008); https://doi.org/10.1016/j.wear.2007.09.005

[5] G. Ma, B. Xu, H. Wang, X. Wang, G. Li, S. Zhang, Surface & Coatings Technology 221, 142 (2013); https://doi.org/10.1016/j.surfcoat.2013.01.039

[6] W. Dai, X. Li, L. Wu, Q. Wang, Diamond & Related Materials 101, 107643 (2020); https://doi.org/10.1016/j.diamond.2019.107643

[7] L. Li, Z. Lu, J. Pu, H. Wang, Q. Li, S. Chen, Z. Zhang, L. Wang, Ceramics International 46(5), 5733 (2020); https://doi.org/10.1016/j.ceramint.2019.11.022

[8] Z. Wang, G. Zhu, F. Lu, L. Zhang, Y. Wang, S. Zhao, C. Guo, J. Zhang, Materials and technology 58(1), 17 (2024); https://doi.org/10.17222/mit.2023.894

[9] H. L. Yang, X. M. Chen, L. Chen, Z. J. Wang, G. C. Hou, C. A. Guo, J. Zhang, Digest Journal of Nanomaterials and Biostructures 18(1), 145 (2023); https://doi.org/10.15251/DJNB.2023.181.145

[10] T. X. Liu, C. A. Guo, F. S. Lu, X. Y. Zhang, L. Zhang, Z. J. Wang, Z. Y. Xu, G. L. Zhu, Chalcogenide Letters 20(10), 741(2023); https://doi.org/10.15251/CL.2023.2010.741

[11] J. Cheng, D. Liu, X. Liang, Y. Chen, Surface and Coatings Technology 281, 109 (2015); https://doi.org/10.1016/j.surfcoat.2015.09.049

[12] A. Leyland, A. Matthews, Wear 246(1-2), 1 (2000); https://doi.org/10.1016/S0043-1648(00)00488-9

[13] L. Ipaz, J. C. Caicedo, J. Esteve, F. J. Espinoza-Beltran, G. Zambrano, Applied Surface Science 258(8), 3805 (2012); https://doi.org/10.1016/j.apsusc.2011.12.033

[14] Q. Wang, M. Chen, Z. Shan, C. Sui, L. Zhang, S. Zhu, F. Wang, Journal of Materials Science & Technology 33(11), 192 (2017); https://doi.org/10.1016/j.jmst.2017.06.014